JTTEE5 15:239-245
DOI: 10.1361/105996306X108156
1059-9630/$19.00 © ASM International

Plasma Sprayed Cast Iron Coatings Containing Solid Lubricant Graphite and h-BN Structure

Y. Tsunekawa, I. Ozdemir, and M. Okumiya

(Submitted August 23, 2005; in revised form December 1, 2005)

Water-atomized cast iron powder of Fe-2.17at.%C-9.93at.%Si-3.75at.%Al were deposited onto an aluminum alloy substrate by atmospheric direct current plasma spraying to improve its tribological properties. Preannealing of the cast iron powder allows the precipitation of considerable amounts of graphite structure in the powder. However, significant reduction in graphitized carbon in cast iron coatings is inevitable after plasma spraying in air atmosphere due to the in-flight burning and dissolution into molten iron droplets. Hexagonal boron nitride (h-BN) powders, which have excellent lubricating properties like graphite, were incorporated into the cast iron powder as a solid lubricant by the sintering process (1300 °C) to obtain protective coatings with a low friction coefficient. The performance of each coating was evaluated using a ring-on-disk-type wear tester under a paraffin-based oil condition in an air atmosphere. A conventional cast iron liner, which had a flaky graphite embedded in the pearlitic matrix, was also tested under similar conditions for comparison. Sections of worn surfaces and debris were characterized, and the wear behavior of plasma-sprayed coatings was discussed.

Keywords atmospheric plasma spray, cast iron coating, friction, graphite, solid lubricant, wear

1. Introduction

Among the many processes used for the surface modification of aluminum alloys, thermal spraying is a promising cost-effective technique that is capable of solving problems such as wear, corrosion, and thermal stability by depositing a relatively thick layer onto a substrate while satisfying the required surface specifications (Ref 1). The most attractive application of spray coatings to aluminum substrates is the surface modification of cylinder bores in automotive industries to reduce the energy loss by the friction and weight loss by the wear, and also to promote lightening of the vehicle (Ref 2-4). Up to now, utilizing many kinds of carbon-based or iron-based powders (Ref 5, 6), the thermal spray modification process, which is capable of depositing a thick coating with a relatively short cycle time to aluminum surfaces, has been used in a wide range of industrial applications, especially in the automotive industry for the realization of linerless cylinder blocks. In addition to these coatings, recently coatings sprayed with cast iron powders, which are relatively inexpensive and exhibit superior wear resistance arising from the graphite structure embedded in the hard matrix, have successfully been applied to modify aluminum alloy surfaces (Ref 7, 8).

The original version of this paper was published in the CD ROM *Thermal Spray Connects: Explore Its Surfacing Potential*, International Thermal Spray Conference, sponsored by DVS, ASM International, and IIW International Institute of Welding, Basel, Switzerland, May 2-4, 2005, DVS-Verlag GmbH, Düsseldorf, Germany.

Y. Tsunekawa and **M. Okumiya,** Toyota Technological Institute, Material Processing Lab, 2-12-1, Hisakata Tempaku, Nagoya, 468-8511, Japan; and **I. Ozdemir,** Dokuz Eylul University, Faculty of Engineering, Department of Metallurgical and Materials Engineering, Bornova, Izmir, 35100, Turkey. Contact e-mail: ismail.ozdemir@deu.edu.tr.

However, the precipitation of graphitized carbon distributed throughout the coating, which provides the necessary wear resistance thanks to a self-lubricating effect, is not a simple process due to the rapid solidification of flattened splats. The preannealing of cast iron powder, and the process of the graphitization and postannealing of coatings are promising approaches to achieving a graphite structure in cast iron coatings except for introducing graphite as a solid lubricant (Ref 8). To achieve reductions in the friction coefficient and wear-loss rate, the introduction of solid lubricants into the coating matrix can be used to produce functional coating, especially for rubbing parts (Ref 9-11). The solid base lubricant materials provide a continual renewable solid lubricant between the mating surfaces during the running-in period, which terminates the local milling action of the abrasive material and reduces the propensity for material flow at the surface. The solid lubricants can be provided as thin films on the surfaces of sliding parts. However, the beneficial effect of the lubricant would disappear due to the reduction in the thickness of the lubricant with an increase in sliding time. Therefore, the incorporation of solid lubricants into starting materials by mechanical mixing, agglomeration, sintering, and spray-drying methods would be expected to yield better tribological behaviors. Because fine solid lubricants distributed within the coating act as oil reservoirs during sliding motion and maintain a self-lubricating effect as the lubricating particles provide continuous lubrication to the sliding surfaces of the parts. However, the content, size, and distribution of the solid lubricant play an important role in obtaining thermally sprayed coatings that exhibit superior wear resistance. Likewise, the wetting condition, adhesion, and interactions of the solid lubricant with the starting material during droplet flight or splat layering have critical influences on wear and friction.

In the present study, water-atomized (WA) cast iron powders containing hexagonal boron nitride (h-BN), which is known as white graphite, offer similar lubrication but are usable at much higher-temperature solid lubricants, and were prepared for at-

Table 1 Chemical composition of water-atomized cast iron powder (wt.%)

	C	O	Si	Mn	P	Al	Fe
WA	2.17	0.35	9.93	0.75	0.96	3.75	bal

mospheric direct current (DC) plasma spraying. The friction and wear performance of the plasma-sprayed cast iron coatings with h-BN structure were studied.

2. Experimental Procedure

The nominal compositions of WA powders for the deposition of plasma-sprayed cast iron coatings are given in Table 1. They contain a strong graphitized element of silicon and aluminum, and a large amount of phosphorus to form steadite. Hexagonal-BN powder of 5 wt.% with a mean particle size of 10 μm were used as a solid lubricant.

Cast iron/h-BN composite powder was prepared by the spray-drying and postsintering method. Figure 1 shows the temperature profile during the heating and cooling periods of the sintering process. The typical appearances of cast iron powder and composite powder after the sintering process are also shown in Fig. 2. It is evident from Table 1 and Fig. 2 that WA powder has high oxygen content and an irregular shape. It is clear that the h-BN powder adhered well to the cast iron surface after the sintering process. A number of h-BN structures are resolvable with scanning electron microscopy (SEM). The base material of atomized cast iron powders is mainly composed of FeSiC, $AlFe_3C_{0.5}$, and χ-FeCSi, which were identified using x-ray diffractometry (XRD) with CoKα radiation. After the sintering process, the WA/h-BN composite powder shows the presence of phases with h-BN and graphite structure. The quantity of graphite was measured by carbon analysis carried out by infrared light absorption during combustion in the oxygen flow. According to the chemical analysis results, graphitized carbon precipitates in the powder at ~1.86 wt.% after the sintering process. Prior to coating deposition, the surfaces of the substrates were grit-blasted with 35-grit alumina using compressed air at a pressure of 4 bar, at a distance of 30 mm, and at an angle of 45°. The surface roughness (R_a) of the aluminum alloy substrates was measured to be 3 μm after 1 min of grit-blasting time, followed by ultrasonic cleaning in acetone. Both powders were then sieved into particle sizes (*dp*) of 32 to 45 μm and were fed into the plasma flame as spray material. Powders were injected in a radial direction by means of a feedstock injector with a diameter of 2 mm.

The standard spray parameters for coating deposition are given in Table 2. Cast iron powder and composite powder were sprayed onto an aluminum alloy substrate (for die casting, Al-11.2wt.%Si-2.74wt.%Cu) kept at room temperature and a constant spray distance. Substrate temperature was continuously recorded through a thermocouple inserted into the center to prevent the substrate from partially melting during the spraying. For this purpose, the substrate was continuously cooled from the backside through an air-cooling nozzle.

The constituent phases of the coatings and rapidly solidified particles, including graphitized carbon and h-BN structures,

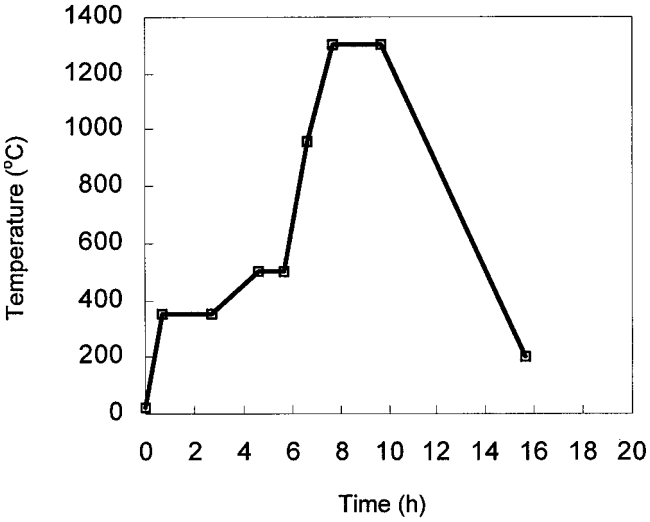

Fig. 1 Temperature profile of powder during the postsintering process after spray-drying

were identified by XRD with a CoKα radiation source and also by a chemical analysis method. Their appearance and cross sections were characterized by optical scanning microscopy and SEM, and elemental distribution was analyzed by an electron probe microanalyzer (EPMA). The Vickers hardness of the coating layers was measured with a load of 2.94 N. The wear and friction experiments of the coatings on rings made of bearing steel (SUJ2; quenched and tempered with 750HV0.3) have been studied using a wear tester with a ring-on-disk configuration. Before performing the test, the surface of the ring and the coating were metallographically prepared to R_a values of 0.28 and 1.44 μm, respectively. The ring dimensions were 25.6 mm for the outer diameter and 20 mm for the inner diameter. Wear tests were carried out keeping the normal force (*Fn*) at 9.4 MPa with paraffin-based oil containing no any additives in an air atmosphere. The rotation speed selected was 0.5 m/s, and the samples were subjected to wear for a total distance for 2000 m. Prior to each test, the working surfaces of the specimens were ground and polished to obtain a similar condition and thickness for the coating layer under test. After the wear tests, the surface profile of the coatings was observed with a Mitutoyo SJ-301 (Kawasaki, Japan) contact profilometer. Sections of worn surfaces and debris were observed by means of light microscopy and SEM. After each test, the wear rates and friction coefficients of the coating layers were determined.

3. Results and Discussion

3.1 Coatings Microstructure

Based on the XRD patterns, the as-atomized powder is composed of FeSiC, $AlFe_3C_{0.5}$, and χ-FeCSi phases, but the graphite structure is not recognized. After the sintering process, in addition to the above phases, graphite and h-BN structures are identified for patterns of WA/h-BN composite powder. The sintering process carried out at 1300 °C leads to the precipitation of graphite in the cast iron powder, level of which is 1.86 wt.% as mea-

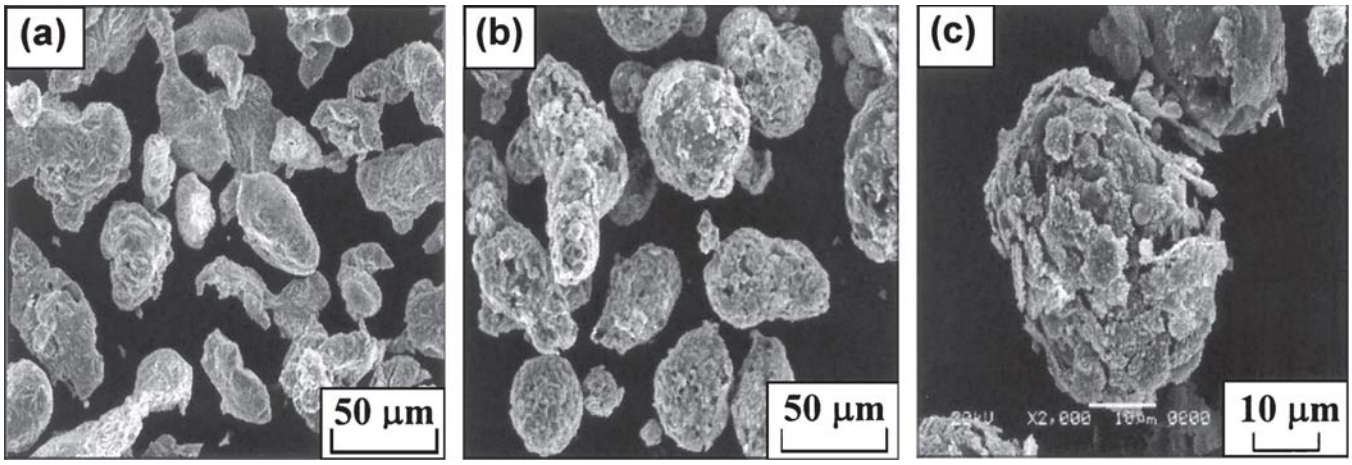

Fig. 2 SEM micrographs showing (a) WA, (b) and (c) WA/h-BN powder particle shapes

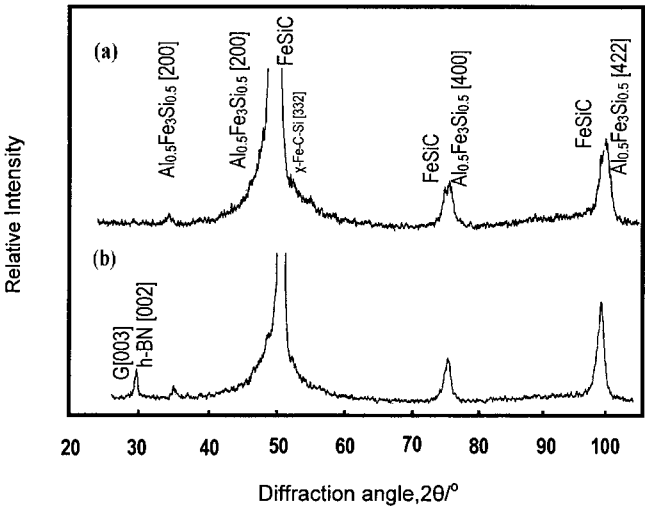

Fig. 3 The XRD patterns of coatings sprayed with (a) as-atomized cast iron powder and (b) WA/h-BN composite powder

Table 2 Standard spray parameters

Parameter	Value
Arc voltage, V	70
Arc current, A	600
Primary gas, m^3/s	Ar: 7.9×10^{-4}
Secondary gas, m^3/s	H_2: 2.4×10^{-6}
Carrier gas, m^3/s	Ar: 1.2×10^{-4}
Spray distance, mm	100
Particle size, μm	$32 < d_p < 45$
Feeding rate, g/min	70

sured by chemical analysis. The as-atomized and WA/h-BN composite powders were plasma-sprayed with the spray parameters given in Table 2. The phase structures of the coatings were analyzed with an x-ray diffractometer. Figure 3 presents the XRD patterns of plasma-sprayed cast iron coatings with as-atomized and WA/h-BN composite powders.

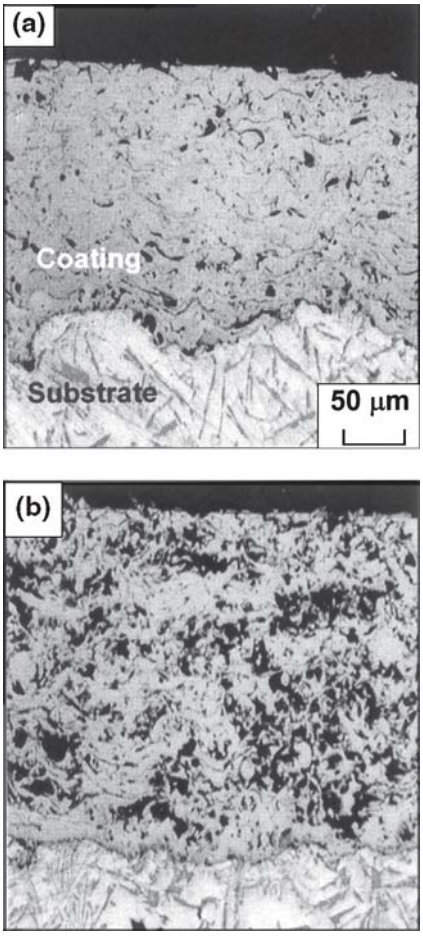

Fig. 4 Cross-section microstructures of the coatings deposited with (a) as-atomized cast iron powder and (b) WA/h-BN composite powder

Based on the XRD results, plasma-sprayed coatings show $Al_{0.5}$ $Fe_3Si_{0.5}$, FeSiC, and χFeCSi as the main constituents. It is also clear that the solid lubricant, h-BN, and the graphite structure were retained in the composite coatings. The typical cross

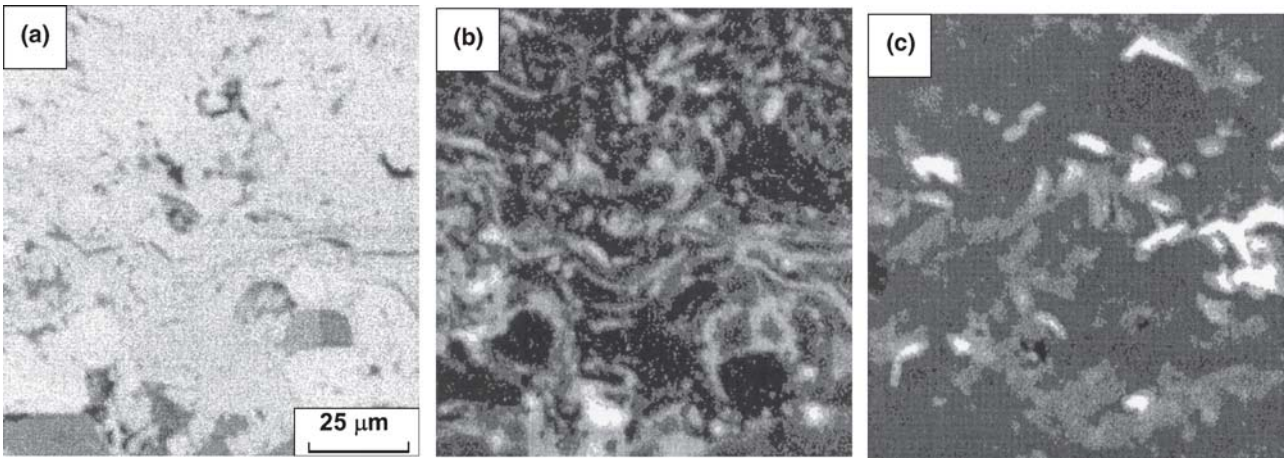

Fig. 5 Characteristic EPMA x-ray images of coating cross sections sprayed with as-atomized powder: (a) BSE image; (b) O-Kα image; and (c) C-Kα image

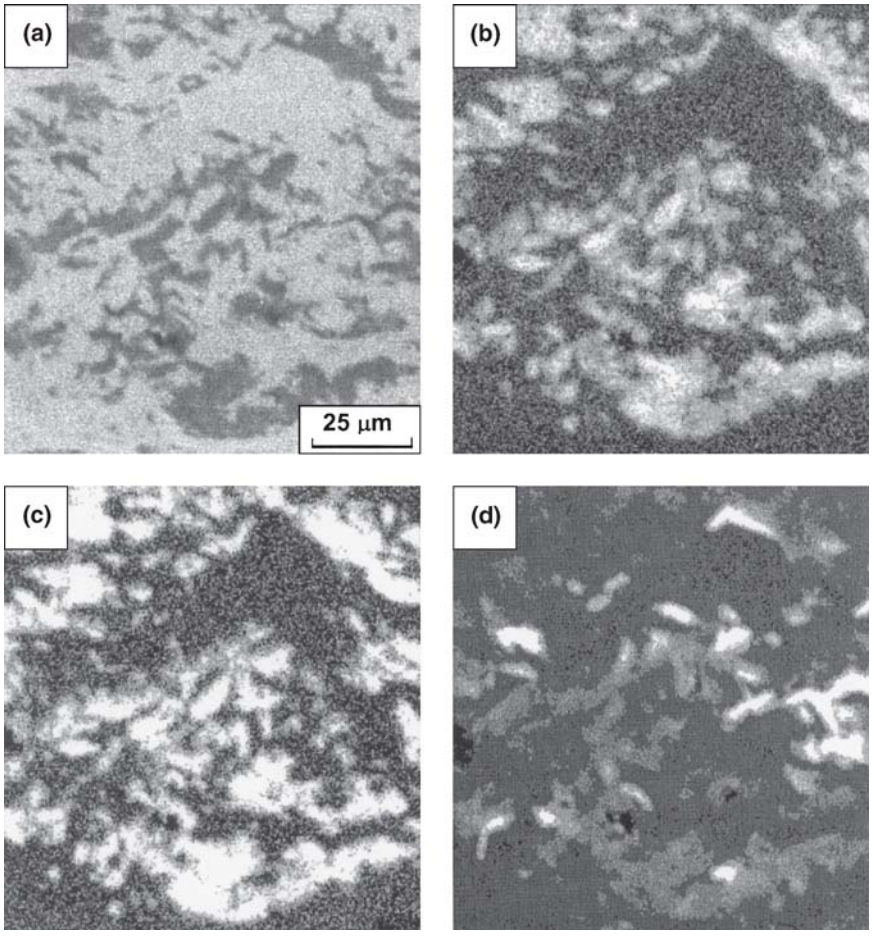

Fig. 6 Element distributions on a cross section of coating sprayed with WA/h-BN composite powder: (a) BSE image; (b) B-Kα image; (c) N-Kα image; and (d) C-Kα image

sections of coatings sprayed with the as-atomized and sintered powder are shown in Fig. 4, in which the coatings exhibit the characteristic wavy, layered structure. The black zones observed in the microstructures, in Fig. 4(b), refer to h-BN and porosity.

All of the cross sections of the coatings were also analyzed by EPMA to determine how the solid lubricant, h-BN, and the graphite were distributed in the sprayed coating. Element mapping by EPMA on the cast-iron coating cross section shown in

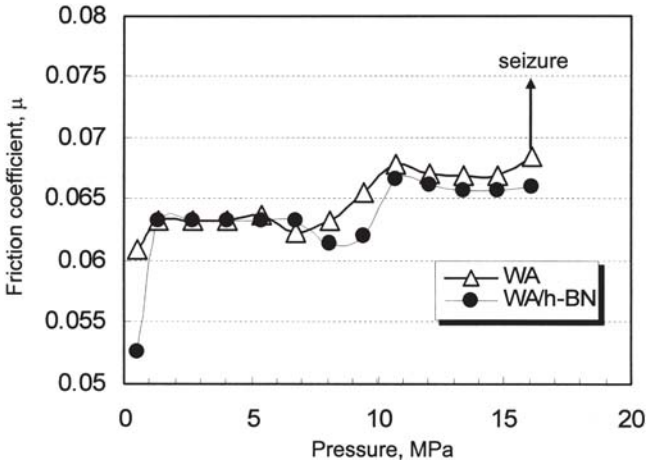

Fig. 7 Change in the friction coefficient of coatings sprayed with as-atomized cast iron powder and WA/h-BN composite powder as a function of contact stress

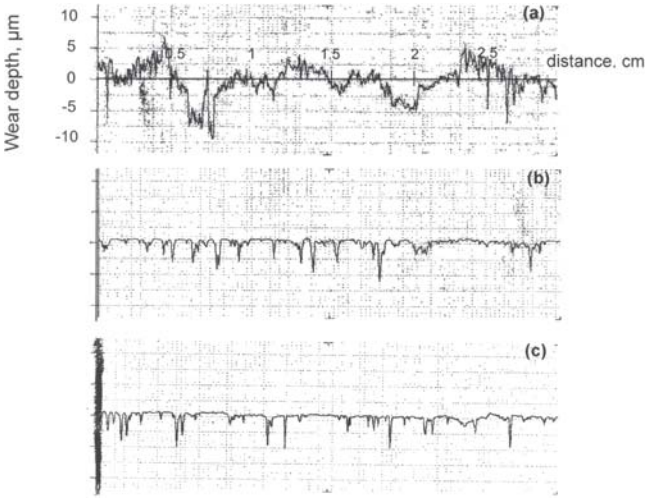

Fig. 8 Surface profiles of (a) cast iron liner, (b) WA, and (c) WA/h-BN sprayed coatings that were wear tested at a load of 9.4 MPa for a sliding distance of 2000 m

Table 3 Friction test conditions

Condition	Value
Sliding speed, m/s	0.5
Load increment rate, MPa/120 s	1.3 MPa/120s
Lubricant	Paraffin-based oil
Ring material	SUJ2 (750 HV0.3)

Fig. 5 revealed the small amounts of the blocky graphite structure based on the C-Kα image, which is not approved by XRD for the coating. The O-Kα indicates that wavy oxide layers are also recognized as black lines in the coating cross section as a result of the in-process oxidation; however, the oxidation level is much lower than that of spraying with bearing steel powder containing low levels of silicon and aluminum. Likewise, the cast iron coating exhibits fewer oxide layers between splats compared with the bearing steel coating, as is shown, qualitatively, by oxygen characteristic x-ray images of EPMA element mapping (Ref 12).

The typical cross section of the coating sprayed with the sintered composite powder, WA/h-BN, which is given in Fig. 6(a), shows the backscattered electron (BSE) image, in which the coating seems to be a layered structure. The dark and gray regions observed in the microstructure possibly contain h-BN solid lubricant and graphite structure, respectively. As a matter of fact, the evidence of h-BN structure through the coating seen in the B-Kα and N-Kα images in Fig. 6(b) and (c), which coincide at high-intensity areas, is clear. The distribution of the solid lubricant phase is relatively homogeneous and well-bonded to the iron-based matrix. The sintering process was carried out to produce a composite powder leading to the formation of a graphite structure in the deposited layers. From the strong C-Kα values seen in Fig. 6(d), the peaks suggest that an appreciable volume fraction of graphite in the structure would be present in the coating. According to the results of chemical analysis, ~1.86 wt.% carbon precipitated in the powder after the sintering process, as mentioned previously. It is worth noting that there is a larger amount of graphite structure retained in the coating sprayed with WA/h-BN powder (1.76 wt.%) compared to that sprayed with the preannealed cast iron powder (0.70 wt.%), which is more prone to in-flight burning due to the relatively large free surface exposed to the plasma flame (Ref 13).

The evaluation of the hardness measurements shows that the coatings sprayed with the as-atomized cast iron and WA/h-BN composite powders exhibit hardness of 444HV0.3 and 274HV0.3, respectively.

3.2 Tribological Performance of Coatings

The cast iron coatings were subjected to the friction test by using a ring-on-disk configuration with a paraffin-based oil lubricant to examine their capability for loading under conditions such as seizure stress. The friction test parameters are given in Table 3. Friction force was measured at different loads and then converted into the friction coefficient. The variation in the friction coefficient with sliding speed v_s = 0.5 m/s are presented in Fig. 7. It can be observed that the coating containing graphitized carbon and h-BN structure has the lowest friction coefficient for the overall trend, which is appreciable especially with increasing load. Even if there is no larger variation in the coefficient of the tested deposits, it was expected that the presence of graphite and h-BN solid lubricant would reduce the friction coefficient and material loss due to their inherent self-lubricating properties. The seizure point shown in Fig. 7 is defined as the maximum load that can be applied on the coating materials such that no severe friction occurs. The results indicate that both types of coatings can be loaded up to a contact pressure of 16 MPa without severe friction, which is beyond the level of the cast iron liner that was previously tested under similar conditions (Ref 8). The wear tests were conducted on polished surfaces of coatings (average R_a 1.44 μm) under the applied constant load of 9.4 MPa for a given sliding distance (2000 m). In all wear tests, no coating loss of the plasma-sprayed coatings was recognized, which was confirmed by means of the roughness tester. This can be attributed to the higher hardness values of the layers (A-WA

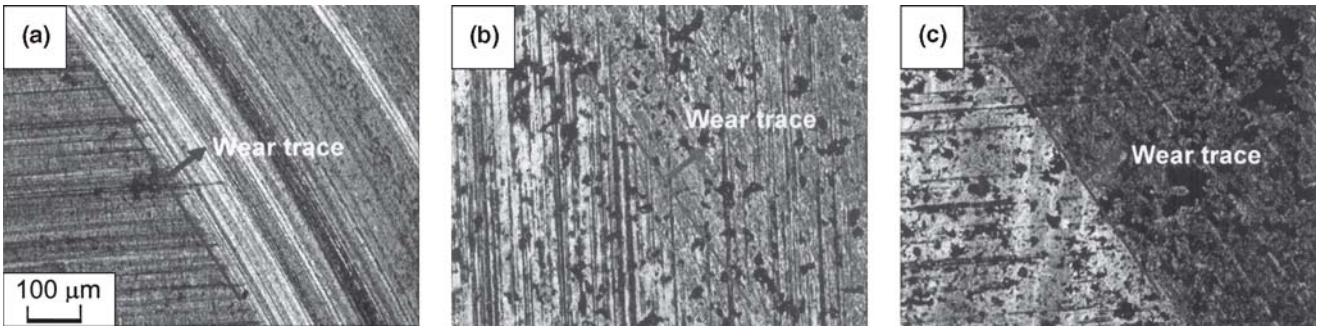

Fig. 9 Optical micrographs showing the morphologies of the worn surfaces of (a) cast iron liner, (b) GA, and (c) WA sprayed cast iron coatings that were tested at a load of 9.4 MPa and a sliding speed of 0.5 m/s

444HV0.3; WA/h-BN 274HV0.3), which prevent the coating layers from penetrating the hard counter body. The typical surface profiles of the coatings before and after the wear test are presented in Fig. 8. It is clear that there is no appreciable increase in wear depth on the worn surfaces. This means that plasma-sprayed coatings remain undeformed under the applied pressure (9.4 MPa) during rotation against a hard bearing steel counterbody. Moreover, compared with the cast iron coatings, the hard counter body (750HV0.3) with a high rotating velocity (0.5 m/s) serves to create a local milling action on the soft cast iron liner (257HV0.3) and causes the formation of longitudinal scratches or microgrooves on its surface, as displayed in Fig. 9(a). It is observable from the surface morphologies of the coatings (Fig. 9b and c) that surface finishing scratches still exist on the wear track of the layers, which proves that no material loss occurred and the layers remained undeformed after wear tests. The worn surface of the coating sprayed with WA/-h-BN, seen in Fig. 9(c), exhibit a different appearance from that of the cast iron coating. The dark regions along the wear track may possibly be a lubricant film that is smeared over the surface of the layers, which might cause a reduction in the friction coefficient values.

Based on these results, it is difficult to conclude that the solid lubricants embedded in the iron-based matrix decrease the friction coefficient values and reduce the wear rate. Because it has been reported that the antiwear performance of the sprayed coatings depends not only on the volume range, size, and distribution of the lubricant in the coatings, but also on the wear behavior of the sprayed deposits, which are affected by a number of factors such as coating hardness, microstructure, bonding quality between the lubricant and the matrix, phase composition, continuity, and the thickness of lubricant film (Ref 14-18). At the least, it can be concluded that the coating containing graphite and h-BN with nearly the same hardness exhibits rather good wear resistance to the hard counterbody of quenched and tempered SUJ.

4. Conclusion

The WA cast iron powder containing high levels of silicon and aluminum and the composite powder produced by sintering the 5 wt.% h-BN solid lubricant were deposited on an aluminum alloy substrate by atmospheric dc plasma spraying. The mechanical properties of the sprayed coatings, such as friction, wear, and hardness, were examined. The main results are summarized as follows:

- The appreciable amount of graphite structure is not identified in cast iron coatings sprayed with as-atomized powders with high silicon and aluminum content, which are known as strong graphitizers in cast iron.
- Sintering cast iron powder at 1300 °C with h-BN powder (5 wt.%) is an applicable method for producing a protective composite coating against friction and wear. After the sintering process, ~1.86 wt.% graphitized carbon precipitates in the cast iron powder and 1.76 wt.% is retained in the coating after plasma spraying.
- Cast iron coatings sprayed with WA and WA/h-BN composite powders show a high seizure point and exhibit good antiwear performance. Both types of coatings show no coating loss in contrast to the cast iron liner. The coatings with relatively low hardness containing a solid lubricant experience the lowest friction coefficient, especially at higher loads, mainly due to the self-lubricating effect.

Acknowledgment

The present work was partially supported by the Grants in Aid for Scientific Research No. 14350404 from the Ministry of Education, Science, Sports and Culture in Japan.

References

1. K. Funatani, M. Yoshida, and Y. Tsunekawa, Surface Modification, Alloy Production and Materials Manufacturing, *Handbook of Aluminium,* Vol. 2, G.E. Totten and D.S. MacKenzie, Ed., 2003, p 536-537
2. F. Kassabji, F. Tourenne, A. Derradji, and P. Fauchais, Aluminum and Aluminum Nitride Deposition by Low Pressure Nitrogen Arc Plasma, *Proceedings of 10th International Thermal Spraying Conference (ITSC),* May 2-6, 1983 (Essen Germany), DVS Berichte, 1983, 82 p
3. R.W. Smith, Reactive Plasma Spray Forming for Advanced Materials Synthesis, *Powder Metall. Int.,* 1993, **25**(1), p 9-16
4. P. Fauchais, A. Vardelle, and A. Denoirjean, Reactive Thermal Plasmas: Ulltrafine Particle Synthesis and Coating Deposition, *Surf. Coat. Technol.,* 1997, **97**(1-3), p 66-78
5. L. Zhao and E. Lugscheider, Reactive plasma spraying of TiAl6V4 alloy, *Wear,* 2002, **253**(11-12), p 1214-1218
6. A. Tronche and P. Fauchais, Frictional Behavior Against Steel of Aluminum Substrates Plasma-Sprayed with Hard Coatings, *Mater. Sci. Eng., A,* 1988, **102**(1), p 1-12
7. Y. Tsunekawa, K. Gotoh, M. Okumiya, and N. Mohri, Synthesis and High-Temperature Stability of Titanium Aluminide Matrix *In-Situ* Composites, *J. Thermal Spray Technol.,* 1992, **1**(3), p 223-229
8. K. Murakami, T. Kawanaka, T. Kujime, and H. Nakajima, Titanium

Aluminides Base Composites with Fine TiB_2 Dispersoids Produced by Reactive Thermal Spraying, *J. High Temp. Soc.,* 1998, **24,** p 200-207
9. Y. Tsunekawa, M. Okumiya, T. Kobayashi, M. Okuda, and M. Fukumoto, Chromium-Nitride *In-Situ* Composites with a Compositional Gradient Formed by Reactive DC Plasma Spraying, *J. Thermal Spray Technol.,* 1996, **5**(2), p 139-144
10. M. Fukumoto, N. Toyama, and I. Okane, Fundamental Study on Synthesis of TiN Coatings by Reactive Plasma Spraying, *J. Japan Thermal Spray Soc.,* 1993, **30**(2), p 54-61
11. Y. Tsunekawa, M. Hiromura, and M. Okumiya, Nitride Formation in Synthesis of Titanium Aluminide Matrix Composite Coatings by Reactive RF Plasma Spraying, *J. Thermal Spray Technol.,* 2000, **9**(1), p 83-89
12. Y. Tsunekawa, M. Okumiya, and A. Kogure, In-Situ Formation of Titanium Carbide by Reactive Plasma Spraying with Elemental Titanium Powder, *Fourteenth International Conference on Surface Modification Technologies,* Sept 11-13, 2000 (Paris, France), Vol 14, 2001, p 10-15
13. J. Lee, L. Ajdelsztajn, N.J. Kim, and E.J. Lavenia, Reactive HVOF Thermal Spraying of Nanocrystalline Ni Powders, *Thermal Spray 2001: New Surfaces for a New Millennium,* C.C. Berndt, K.A. Khor, and E.F. Lugscheider, Ed., May 28-30, 2001 (Singapore), ASM International, 2001, p 511-517
14. Y. Tsunekawa, I. Hamanaka, M. Okumiya, Y. Jung, and M. Fukumoto, Application of In-Process Reaction to the Fabrication of $MgAl_2O_4$/Al-Si Composite Coating by HVOF Spraying, *Fifteenth International Conference on Surface Modification Technologies,* Nov 5-8, 2001 (Indianapolis, IN), 2002, p 9-18
15. P.V. Ananthapadmanabhan and P.R. Taylor, Titanium Carbide-Iron Composite Coatings by Reactive Plasma Spraying of Ilmenite, *J. Alloys Compd.,* 1999, **287**(1-2), p 121-125
16. E. Lugscheider, H. Jungklaus, L. Zhao, and H. Reymann, Reactive Plasma Spraying of Coatings Containing *In-Situ* Synthesized Titanium Hard Phases, *Int. J. Refract. Metals Hard Mater.,* 1997, **15**(5-6), p 311-315
17. K. Funatani, M. Yoshida, and Y. Tsunekawa, Surface Modification, Alloy Production and Materials Manufacturing, *Handbook of Aluminum,* Vol 2, G.E. Totten and D.S. MacKenzie, Ed., 2003, p 536
18. F.M. Morks, Y. Tsunekawa, M. Okumiya, and M. Shoeib, Microstructure of Plasma-Sprayed Cast Iron Splats with Different Particle Sizes, *Mater. Trans.,* 2003, **44**(4), p 743-748